Experimental and Theoretical Investigations of the Bromination of Phenols with *β* and *γ* Aliphatic Substituents, including Rings

Jinsong Zhang,*[,†] Xiao Chang,[†] Erich C. Bowman,[†] Carter J. Holt,[†] Michael W. Lodewyk,*[,†,§] Randy M. Miller,[†] and Guangming Xia*[,†,‡]

[†]Department of Chemistry and Biochemistry, California State University, Chico, California 95929-0210, United States
[‡]School of Chemistry and Chemical Engineering, University of Jinan, Jinan, Shandong 250022, P. R. China

Ⓢ *Supporting Information*

ABSTRACT: Bromination reactions of substituted and ring fused phenols were studied by both experiment (*t*-BuNH-Br) and computation (density functional theory). The outcomes support each other, indicating a clear and predictable regioselective preference among 3,4-bis-alkylated and 3,4-ring-fused phenols.
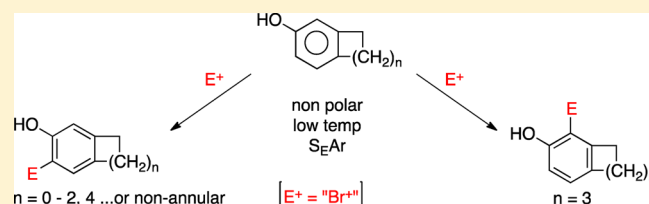
INTRODUCTION

Practitioners of organic synthesis must qualitatively predict a priori the site of an electrophile's reaction with a substituted aromatic ring in order to plan a synthetic strategy. Electron-donating substituents are known to increase the reaction rate for aromatic nucleophiles by activating the ring and increasing the electron density at the corresponding *ortho* and *para* sites.[1] Conversely, electron-withdrawing groups decrease the reaction and deactivating the ring by decreasing the electron density at the *ortho* and *para* sites so as to favor reaction with an electrophile at the *meta* sites.[1] Using this concept, it is usually possible to reason beforehand the preferred site(s) of reaction for a number of simple monocyclic aromatic derivatives. However, as the complexity of the aromatic compound increases by the addition of more substituents, the practitioner must juxtapose a combination of resonance, inductive, and steric effects that can either reinforce or weaken one another at various sites and then decide to what degree these effects matter in the corresponding starting materials, transition states, intermediates, and products.

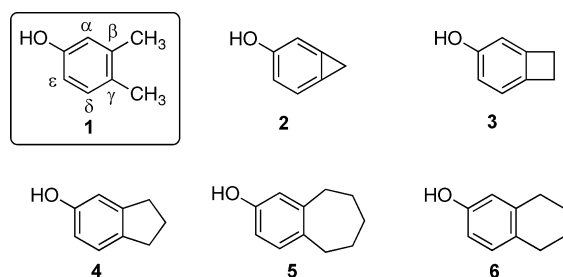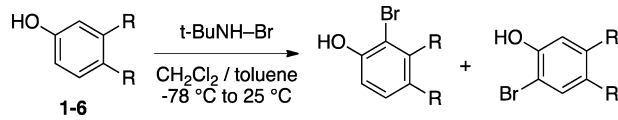Consider 3,4-dimethylphenol (**1**) shown in Figure 1. The phenol substituent strongly directs electrophilic substitution to the *α* and *ε* carbon atoms through resonance, while the less electron-rich *β*-methyl substituent reinforces these reactivity preferences through induction albeit to a lesser extent. The *γ*-methyl substituent, on the other hand, moderately directs electrophiles to the *δ* and *β* carbon atoms through inductive effects. It and its preferential sites can be ignored because the *β* carbon atom is substituted and cannot lead to product, and neither the *β* or *δ* sites are as activated from their neighboring *γ*-methyl residue as the *α* and *ε* sites are from their proximity with the phenol and *β*-methyl residues. Choosing between the *α* and *ε* possibilities for 3,4-dimethylphenol (**1**) becomes a more subtler affair. Inductive effects of the *β*-methyl residue in the phenol **1** would be expected to diminish over distance, making the *α*-site slightly more nucleophilic than the *ε*-site.[2] On the other hand, most practitioners would likely ascribe more steric encumbrance to the *α*-site[3] and thus expect the preponderance of electrophilic aromatic substitution (EAS) to proceed at the unencumbered *ε*-site. Similar lines of reasoning would seem applicable to phenols **2**−**6**, which are fused onto an aliphatic ring at similar *β* and *γ* sites as the methyl substituents in compound **1**.
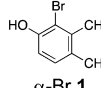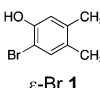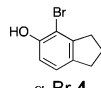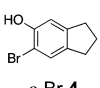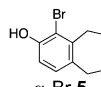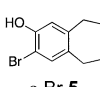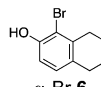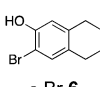
RESULTS AND DISCUSSION

We decided to test these presumptions regarding the regioselective electrophilic aromatic substitution of 3,4-bis-alkylated and ring-fused phenols through a combination of both experiments and calculations. Our modified reaction conditions were anticipated to favor *ortho* substitution over *para*. Our experimental bromination conditions were derived from those originally developed by Pearson[4] and Boozer,[5] which employed *N*-bromo-*tert*-butylamine (*t*-BuNHBr) as both the activating base and source of the Br⁺ electrophile (Table 1). Most speculate that the hydrogen bonding between the nitrogen of

Figure 1. 3,4-Dimethylphenol (**1**) and other phenols fused with aliphatic rings at similar sites (**2**−**6**).

Table 1. Some Experimental Results Regarding Yield and Regioselectivity for Brominations of Phenols 1 and 4−6

Phenol	combined % yield	α-product	ε-product	α : ε ratio[a]
1	66%	α-Br 1	ε-Br 1	23 : 77
4	52%	α-Br 4	ε-Br 4	20 : 80
5	89%	α-Br 5	ε-Br 5	9 : 91
6	60%	α-Br 6	ε-Br 6	97 : 3

[a]Ratio determined by ^{1}H NMR.

the N-bromo-tert-butylamine and the phenol hydrogen leads to a cyclic transition state that favors ortho delivery of the bromonium.[6] The starting phenols **1**, **4**, and **6** were commercially available. The cycl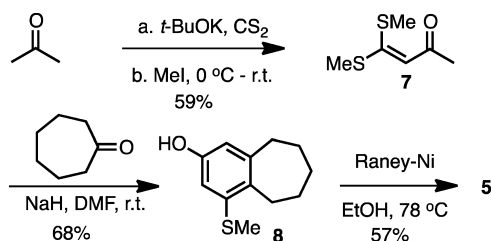oheptane-fused phenol **5** was prepared according to our modification of the procedures independently developed and reported by both Barun and Potts (Scheme 1).[7,8] While not experimentally tested by reaction due to strain, the theoretical outcome of the phenols **2** and **3** were examined by calculation.

Scheme 1

Under the experimental bromination conditions denoted, 3,4-dimethylphenol (**1**) was observed to afford a 23:77 ratio (α-Br **1**/ε-Br **1**) in a 66% combined yield. The indanol **4** was observed to undergo preferential reaction at the ε-site affording a 20:80 ratio (α-Br **4**/ε-Br **4**) in a 52% combined yield. The phenol **5**, which is fused with a seven-membered ring, was also found to favor addition at the ε-site resulting in a 9:91 ratio (α-Br **5**/ε-Br **5**) in a 89% combined yield. On the other hand, the tetralinol **6** was shown to undergo bromonium addition at its α-site proceeding in a 97:3 ratio (α-Br **6**/ε-Br **6**) in a 60% combined yield.

■ THEORETICAL CALCULATIONS

Next, we carried out a comprehensive theoretical study to further illuminate the origins of the α and ε regioselectivity for

bromination of the phenols **1−6**. Using density functional theory, we calculated the gas-phase relative energy and differences for the final brominated products as well as pertinent transition states and ground-state energies for reaction intermediates surrounding the rate-determining step along the reaction coordinate (Figure 2).

Calculative comparisons of the ground-state energy for the final α- and ε-brominated products were in qualitative agreement with the experimentally observed (α: ε) ratio for brominated products **1**, **5**, and **6**, but not **4** (Table 2). Subtraction of respective ground-state energies indicate that the α-Br products arising from compounds **2**, **3**, **4**, and **6** are more stable than their corresponding ε-isomers by 0.40−1.06 kcal/mol in the gas phase. On the other hand, similar comparisons of ground-state energies show the ε-bromination products arising from dimethylphenol (**1**) and the phenol **5** are more stable than their corresponding α-isomer. An obvious explanation for these energetic differences among the ground-state energies of the final products and their respective magnitudes was not apparent to us from simple considerations of steric and strain effects. However, considering that the reaction is most likely under kinetic control as opposed to thermodynamic control, we set out to calculate the ground-state energies of the respective cyclohexadienone intermediates as well as their preceding transition states involved in the rate-determining endothermic step.

The comparison of ground-state energies among the respective isomeric brominated α- and ε-cyclohexadienone intermediates for phenols **1−6** proved to be very informative and to closely reflect our experimental findings shown in Table 1. Calculations showed that the ε-brominated cyclohexadienone intermediates were more stable than their corresponding α-brominated cyclohexadienone intermediates for the starting phenols **1−5** (Table 3). The relative order of ε-regioselectivity was predicted to be **2 > 3 > 5 > 1 ≈ 4**, which closely mirrored our earlier experiments. Remarkably, the similar differences calculated for both phenols **1** and **4**, 0.57 kcal/mol for each, corresponded nicely with the similar isomeric ratios of 23:77 and 20:80 we had observed. Moreover, the larger ε to α energy difference for the seven-membered phenol **5** appears to be evident in its larger (9:91 α/ε) experimental ratio as compared to calculations and experimental results for phenols **1** and **4**. In addition, the calculative comparisons of the α- and ε-brominated cyclohexadienone intermediates arising from phenol **6** indicate the α brominated cyclohexadienone to be considerably more stable than its ε-isomer. This calculation appears to be substantiated by the direction and magnitude observed in the (97:3 α/ε) bromination ratio for phenol **6** in Table 1. Although not experimentally tested, the calculation of the ground-state energies of the respective brominated cyclohexadienone intermediates for the phenols **2** and **3** suggests the greater preponderance of the ε-product over the α-product.

The transition-state structures for the RDS were calculated for each regioisomer and confirmed by the analysis of the imaginary frequencies and by Intrinsic Reaction Coordinate (IRC) calculations. Figure 3 shows the anticipated geometries along with bond lengths in angstroms for the starting phenol **4** and its respective α and ε transition states. Comparisons among the relative outputted energies for the α and ε TS‡ predicted that the ε-brominated TS‡ to be more stable and, hence, preferred over the α-brominated products of phenols **1−5** as well as the preponderance of the α-product upon bromination
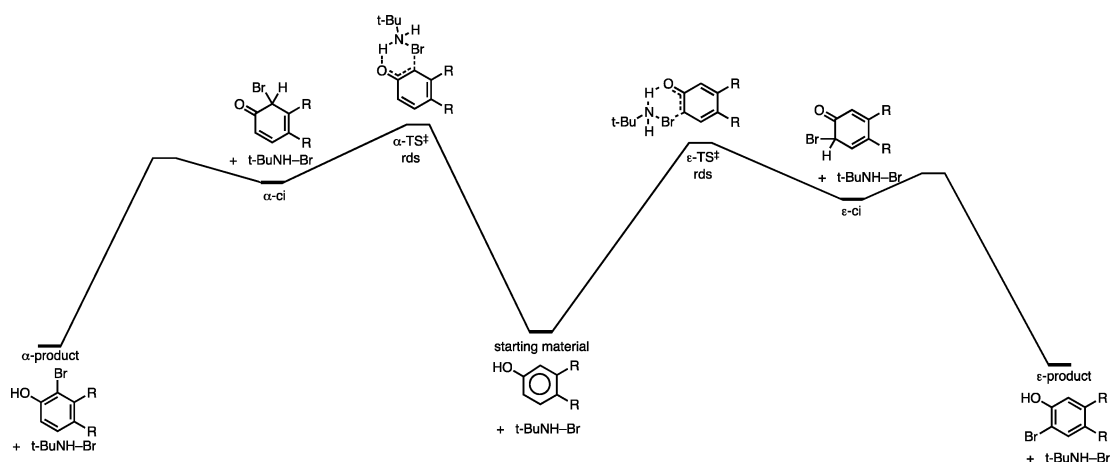
Figure 2. Reaction coordinate for bromination at α and ε sites of 3,4-bis-alkylated and ring-fused phenols (ci: cyclohexadienone intermediate).

Table 2. Computed Relative Energies (kcal/mol) for α- and ε-Brominated Phenols

starting material	ΔE^a		$\Delta E, \alpha - \varepsilon$
	α-product	ε-product	
1	α-Br **1**, −18.99	ε-Br **1**, −19.78	+0.79e
2	α-Br **2**, −20.30	ε-Br **2**, −19.24	−1.06a
3	α-Br **3**, −20.19	ε-Br **3**, −19.51	−0.68a
4	α-Br **4**, −20.59	ε-Br **4**, −19.74	−0.85a
5	α-Br **5**, −18.77	ε-Br **5**, −19.86	+1.09e
6	α-Br **6**, −20.20	ε-Br **6**, −19.80	−0.40a

[a]Computed (electronic energy + ZPE correction) relative to starting substrate. Computed values for the starting material include the energy of N-bromo-tert-butylamine and intermediates, and products include the energy of tert-butylamine computed as an isolated structure.

Table 3. Computed Energies (kcal/mol) for α- and ε-Brominated Cyclohexadienone Intermediates

starting material	ΔE^a		$\Delta E, \alpha - \varepsilon$
	α-ci	ε-ci	
1	−1.93	−2.50	+0.57
2	−1.45	−6.72	+5.27
3	−1.98	−4.44	+2.46
4	−2.67	−3.24	+0.57
5	−1.87	−2.53	+0.66
6	−4.05	−1.57	−2.48

[a]Computed (electronic energy + ZPE correction) relative to starting substrate. Computed values for the starting material include the energy of N-bromo-tert-butylamine and intermediates, and products include the energy of tert-butylamine computed as an isolated structure. ci: cyclohexadienone intermediate.
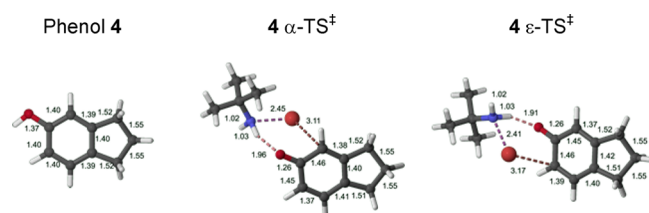
Figure 3. Computed geometries and bond lengths.

of the phenol **6** (Table 4). However, magnitude of the calculated differences did not correspond as well with the

Table 4. Transition State Barriers (kcal/mol) for RDS Leading to α and ε Products

starting material	$\Delta E^{\ddagger a}$		$\Delta E^{\ddagger}, \alpha - \varepsilon$
	α-TS‡	ε-TS‡	
1	22.28	22.11	0.17
2	21.61	20.68	0.93
3	21.84	21.48	0.36
4	21.85	21.74	0.11
5	22.11	22.07	0.04
6	21.93	22.30	−0.37

[a]Computed (electronic energy + ZPE correction) relative to starting substrate. Computed values for the starting material include the energy of N-bromo-tert-butylamine and intermediates, and products include the energy of tert-butylamine computed as an isolated structure. ci: cyclohexadienone intermediate.

experimentally observed regioisomer ratios. For example, the relative order of ε-regioselectivity among the starting phenols for the bromination reaction was predicted to be **2** > **3** > **1** > **4** > **5**. Experimental bromination of the phenol **5** afforded measurably more of the ε-brominated product than found for the phenols **1** or **4**. Upon closer inspection of our models, which showed increased bond alteration around the phenol ring, it is evident that the transition states displayed partial loss of aromaticity (Figure 3). Moreover, as the breaking N–Br and O–H bonds appeared to be slightly shorter and the forming C–Br bond appeared to be slightly longer, we concluded that the ε transition state occurred earlier than the corresponding α transition state. Therefore, in order to better illuminate how the aromatic character might affect the product ratio, we chose to employ NICS (nucleus independent chemical shift) calculations[9] in the hopes of finding a better correlation of calculations with the regioisomeric ratios obtained by experiment.

For each phenol reactant and its corresponding α and ε transition states, the chemical shift at the centroid of the ring, NICS-(0), was computed along with chemical shifts 1 Å above and below the centroid, NICS-(1) (Table 5). These numbers indicate the degree of shielding, and thus aromaticity; a more negative value indicates a greater degree of aromaticity. Thus, with a NICS-(0) = −10.65, phenol **3** appears to be most aromatic, whereas phenol **2** with a NICS-(0) = −9.79 appears to be the least aromatic. It is known that NICS-(0) is somewhat affected by σ-bond effects, whereas measurements 1 Å above

Table 5. NICS Values Computed for Reactants and Transition States

phenol		NICS-(0)	NICS-(1)			NICS-(0)	NICS-(1)	
			1 Å below	1 Å above			1 Å below	1 Å above
1	reactant	−10.48	−10.67	−10.66	reactant	−10.48	−10.67	−10.66
	α-TS‡	−0.01	−3.91	−4.26	ε-TS‡	−0.36	−4.55	−4.12
	$\Delta\delta_{\alpha}$	+10.47	+6.76	+6.40	$\Delta\delta\varepsilon$	+10.12	+6.12	+6.55
2	reactant	−9.79	−10.85	−10.84	reactant	−9.79	−10.85	−10.84
	α-TS‡	+0.64	−4.50	−4.85	ε-TS‡	−1.30	−5.89	−5.46
	$\Delta\delta_{\alpha}$	+10.43	+6.35	+5.99	$\Delta\delta\varepsilon$	+8.49	+4.96	+5.38
3	reactant	−10.65	−10.46	−10.46	reactant	−10.65	−10.46	−10.46
	α-TS‡	−0.05	−3.68	−4.03	ε-TS‡	−1.17	−4.33	−4.72
	$\Delta\delta_{\alpha}$	+10.60	+6.78	6.43	$\Delta\delta\varepsilon$	+9.48	+6.13	+5.74
4	reactant	−10.01	−10.53	−10.24	reactant	−10.01	−10.53	−10.24
	α-TS‡	+0.16	−3.79	−4.23	ε-TS‡	−0.47	−4.73	−4.14
	$\Delta\delta_{\alpha}$	10.17	6.74	6.01	$\Delta\delta\varepsilon$	+9.54	+5.80	+6.10
5	reactant	−10.45	+10.53	−10.65	reactant	−10.45	+10.53	−10.65
	α-TS‡	−0.25	−3.95	−4.34	ε-TS‡	−0.47	−4.51	−4.21
	$\Delta\delta_{\alpha}$	+10.20	+6.57	6.31	$\Delta\delta\varepsilon$	+9.98	+6.02	+6.44
6	reactant	−10.07	−10.35	−10.33	reactant	−10.07	−10.35	−10.33
	α-TS‡	−0.17	−3.91	−4.25	ε-TS‡	0.00	−4.26	−3.89
	$\Delta\delta_{\alpha}$	+9.90	+6.43	6.08	$\Delta\delta\varepsilon$	+10.07	6.08	6.45

and below the centroid are not.[9] For comparison, at the B3LYP/6-31G(d) level of theory, benzene has a computed NICS-(0) value of −9.65 ppm and a NICS-(1) value of −11.22 ppm.

For each reactant except phenol **2**, the computed NICS-(0) values are between −10 and −11 ppm, whereas the values for the transition-state structures span a ∼5 ppm range. Notably, for phenols **1−5**, the transition-state structures with the smaller NICS-(0) $\Delta\delta$ values (less loss of aromaticity) correspond to the experimentally observed major product (see Table 1) and the DFT calculated preference to the ε-products. The smaller $\Delta\delta$ values can be taken as further evidence of earlier transition-state structures in these exothermic reaction steps and thus are in line with the lower computed energy barriers. On the other hand, only 70% of the NICS-(1) (including both sides of the ring) predict the experimentally observed major product. For the phenol **6**, the NICS-(0) and one of the NICS-(1) correspond to the experimental and DFT data.

CONCLUSION

According to the computational study, the experimental regioselectivity is due to an interplay of aromaticity of the benzene fragment and the angular strain of the aliphatic ring. It is essentially related to the transition states of each individual reaction. The regioselectivity supports a broad Mills-Nixon effect.[10] Despite the limited development of physical organic chemistry in early 20th century, the Mills-Nixon effect has been and is still a subject of long-standing research interest, debates and misunderstanding.[11,12] Maksic recently defined the Mills-Nixon effect as "a perturbation of the aromatic moiety exerted by fusion of one (or several) nonaromatic angularly strained molecules." Regioselective syntheses based on the Mills-Nixon effect have been applied widely in organic and natural product synthesis.[13−16]

EXPERIMENTAL SECTION

General Methods. In all reactions, where water was not present as solvent, reagent, or a byproduct, the reaction vessels were dried in an oven. In addition, the reactions were conducted under a slight positive pressure of dry argon during the course of the reaction. All reactions were monitored by analytical thin-layer chromatography using hard layer silica gel 60^{F-250} plates. Visualization was effected by ultraviolet light (254 nm), followed by staining the plate and drying with heat. All reactions were stirred with Teflon-coated magnetic stir bars. Solvents were typically removed using a rotary evaporator connected to vacuum pump. All commercially available reagents were used without purification unless otherwise noted. Low-boiling solvents were distilled before use under a slight positive pressure of argon. ^{1}H NMR spectra were recorded on 300 MHz spectrometer. Chemical shifts are reported in ppm from tetramethylsilane with the solvent resonance of CDCl$_3$ (7.26 ppm).

General Procedure in Preparing _N_-Bromo-_tert_-butylamine. Freshly distilled _tert_-butylamine (0.04 mol) was mixed with sodium hydroxide solution (10 M, 4 mL) and 10 mL of water in a round-bottom flask with a stir bar. Bromine (0.04 mol) was added dropwise, and the reaction mixture was stirred at 0−5 °C. Ten minutes after the bromine was added, the reaction mixture was extracted with diethyl ether (3 × 20 mL). The organic layer was dried over magnesium sulfate, filtered, and then condensed using a rotary evaporator. _N_-Bromo-_tert_-butylamine is a deep red-orange liquid and should be used immediately because it could decompose to _tert_-butylamine hydrobromide.

Preparation of the Phenol 5. The phenol **5** was prepared in three steps with acetone (2.20 mL, 1.74 g, 30 mmol) and carbon disulfide (1.81 mL, 2.28 g, 30 mmol) as starting materials and an overall yield of 23% (1.11g).[7,8]

General Procedure for Phenol Bromination. Four equivalents of a freshly prepared (0.4 M) toluene solution of _N_-bromo-_tert_-butylamine was added dropwise to a solution of the respective phenol (0.7 M in methylene chloride) with stirring at −78 °C. The reaction was then permitted to slowly warm to room temperature over 1−2 h while being carefully monitored at 5 min intervals by GC/MS. As soon as bis-bromination could be first detected, the reaction was then quenched with water and the aqueous layer separated and discarded. Sodium hydroxide (10%) was then added, the reaction mixture was separated, and the organic layer was discarded. After acidification, the remaining aqueous layer was acidified with 1 N HCl and extracted two times with methylene chloride, and the combined organic extracts were then dried over magnesium sulfate, filtered, and finally condensed with rotary evaporator. The crude product mixture was then analyzed with GC/MS so that a ratio of the regioisomers could be determined. An ^{1}H NMR spectrum was taken of these respective crude product mixtures so that the favored regioisomer might be distinguished by analysis of proton coupling; the α-H singlet among ε-Br products and

the ε-H a doublet among α-Br products. The crude product was then purified by flash chromatography with silica gel eluting with 10:1 hexane/ethyl acetate or 20:1 hexane/chloroform so that a yield of the mixture could be determined.

2-Bromo-3,4-dimethylphenol (α-Br 1): pale yellow solid; ^{1}H NMR (300 MHz; CDCl$_3$) δ 6.99 (d, J = 8.2 Hz, 1H), 6.79 (d, J = 10.6 Hz, 1H), 5.47 (s, 1H), 2.36 (s, 3H), 2.26 (s, 3H).

2-Bromo-4,5-dimethylphenol (ε-Br 1): pale yellow solid; ^{1}H NMR (300 MHz; CDCl$_3$) δ 7.20 (s, 1H), 6.82 (s, 1H), 5.25 (s, 1H), 2.18 (s, 3H), 2.17 (s, 3H).

4-Bromo-2,3-dihydro-1H-inden-5-ol (α-Br 4): pale yellow solid; ^{1}H NMR (300 MHz; CDCl$_3$) δ 7.03 (d, J = 7.6, 1H), 6.80 (d, J = 7.6, 1H), 5.74 (s, 1H), 1.92 (m, 4H), 2.11 (m, 2H).

6-Bromo-2,3-dihydro-1H-inden-5-ol (ε-Br 4): pale yellow solid; ^{1}H NMR (300 MHz; CDCl$_3$) δ 7.28 (s, 1H), 6.89 (s, 1H), 5.35 (s, 1H), 2.83 (m, 4H), 2.18 (m, 2H).

1-Bromo-6,7,8,9-tetrahydro-5H-benzo[7]annulen-2-ol (α-Br 5): pale yellow solid; ^{1}H NMR (300 MHz; CDCl$_3$) δ 6.94 (d, J = 7.6, 1H), 6.76 (d, J = 8.2, 1H), 5.51 (s, 1H), 2.70–2.67 (m, 4H), 1.80–1.59 (m, 6H).

3-Bromo-6,7,8,9-tetrahydro-5H-benzo[7]annulen-2-ol (ε-Br 5): pale yellow solid; ^{1}H NMR (300 MHz; CDCl$_3$) δ 7.16 (s, 1H), 6.78 (s, 1H), 5.27 (s, 1H), 2.70–2.67 (m, 4H), 1.80–1.59 (m, 6H).

1-Bromo-5,6,7,8-tetrahydronaphthalen-2-ol (α-Br 6): white crystalline solid; ^{1}H NMR (300 MHz; CDCl$_3$) δ 6.95 (d, J = 8.2, 1H), 6.82 (d, J = 8.2, 1H), 5.52 (s, 1H), 2.72 (m, 4H), 1.75 (m, 4H).

3-Bromo-5,6,7,8-tetrahydronaphthalen-2-ol (ε-Br 6): white crystalline solid; ^{1}H NMR (300 MHz; CDCl$_3$) δ 7.16 (s, 1H), 6.74 (s, 1H), 5.80 (s, 1H), 2.72 (m, 4H), 1.75 (m, 4H).

Computational Methods. Quantum mechanical calculations were performed with GAUSSIAN03.[17] All calculations (optimizations, frequencies, and NICS) were performed in the gas phase using the B3LYP/6-31G(d) level of theory.[18−22] NMR single-point calculations for the NICS values utilized the default GIAO method.[23−27]

■ ASSOCIATED CONTENT

ⓢ Supporting Information

The Supporting Information is available free of charge on the ACS Publications website at DOI: 10.1021/acs.joc.5b01866.

^{1}H NMR spectra and all data emerging from quantum mechanical calculations (PDF)

■ AUTHOR INFORMATION

Corresponding Authors
*E-mail: jzhang2@csuchico.edu.
*E-mail: lodewykmi@butte.edu.
*E-mail: xiagm@hotmail.com.

Present Address
§Physical Science Department, Butte College, Oroville, CA 95965.

Notes
The authors declare no competing financial interest.

■ ACKNOWLEDGMENTS

■ REFERENCES

(1) Hoggett, J. G.; Moodie, R. B.; Penton, J. R.; Schofield, K. *Nitration and Aromatic Reactivity*; Cambridge University Press: Cambridge, 1971.
(2) Groves, L. G.; Baker, J. W. *J. Chem. Soc.* **1939**, 1144−1150.
(3) Kruse, L. I.; cha, J. K. *J. Chem. Soc., Chem. Commun.* **1982**, 1333−1336.
(4) Pearson, D. E.; Wysong, R. D.; Breder, C. V. *J. Org. Chem.* **1967**, 32, 2358−2360.
(5) Boozer, C. E.; Moncrief, J. W. *J. Org. Chem.* **1962**, 27 (2), 623−624.
(6) Dukker, L. J. Ph.D. Thesis, University of Leiden, Leiden, The Netherlands, 1964.
(7) Barun, O.; Nandi, S.; Panda, K.; Ila, H.; Junjappa, H. *J. Org. Chem.* **2002**, 67 (15), 5398−5401.
(8) Potts, K. T.; Winslow, P. A. *Synthesis* **1987**, 1987, 839−841.
(9) Chen, Z.; Wannere, C. S.; Corminboeuf, C.; Puchta, R.; Schleyer, P. v. R. *Chem. Rev.* **2005**, 105, 3842−3888.
(10) Mills, H. W.; Nixon, I. G. *J. Chem. Soc.* **1930**, 2510−2524.
(11) Eckert-Maksic, M.; Glasovac, Z.; Coumbassa, N. N.; Maksic, Z. B. *J. Chem. Soc., Perkin Trans. 2* **2001**, 1091−1098.
(12) Lange, J.; Hoogenveen, S.; Veerman, W.; Wals, H. *Heterocycles* **2000**, 53, 197−204.
(13) Huang, Y.; Zhang, J.; Pettus, T. R. R. *Org. Lett.* **2005**, 7, 5841−5844.
(14) Touzeau, F.; Arrault, A.; Guilaumet, G.; Scalbert, E.; Pfeiffer, B.; Rettori, M.; Renard, P.; Merour, J. Y. *J. Med. Chem.* **2003**, 46, 1962−1979.
(15) Andreetti, G. D.; Bohmer, V.; Jordon, J. G.; Tabatabai, M.; Ugozzoli, F.; Vogt, W.; Wolff, A. *J. Org. Chem.* **1993**, 58, 4023−4032.
(16) Singh, V.; Sahu, P. K.; Singh, R. B.; Mobin, S. M. *J. Org. Chem.* **2007**, 72, 10155−10165.
(17) Frisch, M. J. et al., Gaussian 03, Revision D.01, Gaussian, Inc., Wallingford, CT, 2004. The full citation is provided in the Supporting Information.
(18) Becke, A. D. *J. Chem. Phys.* **1993**, 98, 1372−1377.
(19) Becke, A. D. *J. Chem. Phys.* **1993**, 98, 5648−5652.
(20) Lee, C.; Yang, W.; Parr, R. G. *Phys. Rev. B: Condens. Matter Mater. Phys.* **1988**, 37, 785−789.
(21) Stephens, P. J.; Devlin, F. J.; Chabalowski, C. F.; Frisch, M. J. *J. Phys. Chem.* **1994**, 98, 11623−11627.
(22) Tirado-Rives, J.; Jorgensen, W. L. *J. Chem. Theory Comput.* **2008**, 4, 297−306.
(23) London, F. *J. Phys. Radium* **1937**, 8, 397−409.
(24) McWeeny, R. *Phys. Rev.* **1962**, 126, 1028−1034.
(25) Ditchfield, R. *Mol. Phys.* **1974**, 27, 789−807.
(26) Wolinski, K.; Hilton, J. F.; Pulay, P. *J. Am. Chem. Soc.* **1990**, 112, 8251−8260.
(27) Cheeseman, J. R.; Trucks, G. W.; Keith, T. A.; Frisch, M. J. *J. Chem. Phys.* **1996**, 104, 5497−5509.